

Available online at [www.sciencedirect.com](http://www.sciencedirect.com)

ScienceDirect

journal homepage: [www.e-jds.com](http://www.e-jds.com)

Original Article

# Involvement of endoplasmic reticulum stress and cell death by synthesized Pa-PDT in oral squamous cell carcinoma cells

Hyo-Eun Yoon <sup>a†</sup>, Mee-Young Ahn <sup>b†</sup>, Yong-Chul Kim <sup>c</sup>,  
Jung-Hoon Yoon <sup>a\*</sup>



<sup>a</sup> Department of Oral and Maxillofacial Pathology, College of Dentistry, Wonkwang Dental Research Institute, Daejeon Dental Hospital, Wonkwang University, Daejeon, Republic of Korea

<sup>b</sup> Department of Pharmaceutical Engineering, College of Health and Welfare, Silla University, Busan, Republic of Korea

<sup>c</sup> Department of Life Sciences, Gwangju Institute of Science and Technology, Gwangju, Republic of Korea

Received 24 November 2021; Final revision received 10 February 2022

Available online 1 March 2022

## KEYWORDS

Pa-PDT;  
ER stress;  
Oral squamous cell carcinoma;  
Apoptosis;  
Autophagy

**Abstract** *Background/purpose:* Photodynamic therapy (PDT) is a therapeutic alternative for malignant tumors that uses a photosensitizer. This study examined whether synthesized Pheophorbide a (Pa)-PDT induced apoptosis and autophagy involving endoplasmic reticulum (ER) stress in oral squamous cell carcinoma (OSCC) cells.

*Materials and methods:* Human OSCC cells were treated with Pa-PDT, and cell proliferation was examined by MTT assay. Apoptosis and autophagy were measured using Western blot analysis. ER stress was examined using RT-PCR and Western blot analysis. In vivo murine OSCC animal model were treated with intratumoral (IT) Pa-PDT, and investigated the therapeutic effect.

*Results:* Pa-PDT significantly inhibited the proliferation of human OSCC cells in a dose-dependent manner. Pa-PDT induced intrinsic apoptotic cell death and also induced autophagy. Pa-PDT induced ER stress which was observed as demonstrated by the up-regulation of the ER stress marker. Inhibition of the ER stress pathway using 4-phenylbutyric acid (PBA) decreased CHOP and induced inhibition of cell deaths. In addition, the inhibition of ER stress enhanced Pa-PDT mediated autophagy. IT Pa-PDT significantly inhibited the tumor growth and induced apoptosis, autophagy and ER stress in vivo OSCC cells transplanted model.

*Conclusion:* This study showed that synthesized Pa-PDT induced ER stress trigger apoptosis and apoptotic cell death pathways in OSCC cells. The inhibition of ER stress declined Pa-PDT

\* Corresponding author. Department of Oral and Maxillofacial Pathology, College of Dentistry, Wonkwang University, Daejeon, 35233, Republic of Korea. Fax: +82 42 366 1115

E-mail address: [opathyoon@wku.ac.kr](mailto:opathyoon@wku.ac.kr) (J.-H. Yoon).

† These authors contributed equally to this work.

mediated cytotoxicity with an increase of autophagy. These results may provide Pa-PDT exerts anti-tumor effects through ER stress pathway in OSCC cells and may provide a basis for developing Pa-PDT targeting ER stress as a therapy for OSCC.

© 2022 Association for Dental Sciences of the Republic of China. Publishing services by Elsevier B.V. This is an open access article under the CC BY-NC-ND license (<http://creativecommons.org/licenses/by-nc-nd/4.0/>).

## Introduction

Photodynamic therapy (PDT) is a method that causes membrane damage and oxidative stress in cells through light irradiation of the photosensitizer, which leads to cell death eventually causing tumor destruction.<sup>1</sup> PDT is a nonsurgical alternative for the treatment of several diseases and a potent treatment option for patients suffering from early oral cancer and advanced head and neck cancer.<sup>2,3</sup> The photosensitizer is one of the important components of determining PDT efficacy. Many new compounds have been synthesized to improve some limitation of the first photosensitizer Photofrin such as poor water solubility, lack of absorption in long wavelength, and takes a long time to be excreted from the body.<sup>4,5</sup> In particular Pheophorbide a (Pa), one of the products derived from chlorophyll degradation, has attracted widespread attention in recent years as a non-invasive and highly selective approach for cancer treatment. Recently, You et al. synthesized Pa by removing magnesium ion from chlorophyll-a and hydrolysis with 80% TFA.<sup>6</sup>

Endoplasmic reticulum (ER) stress can affect cellular stability, leading to viral infections, oxidative stress, decreased ER calcium levels, and abnormal protein folding.<sup>7,8</sup> ER stress activates a signaling pathway called the unfolded protein response (UPR).<sup>9</sup> Three ER-related mechanisms have been found to be responsible for mediating the UPR of eukaryotes (i.e. activating transcription factor 6 (ATF6), inositol-requiring enzyme 1 (IRE1), PKR-like ER kinase (PERK)).<sup>9,10</sup> These mechanisms are governed predominantly by the intensity of ER stress which can switch between pro-survival and pro-death signaling. However, no clear conclusion has been reached on the correlation of ER stress and apoptosis or autophagy especially in the case of PDT-induced cell death.

Oral squamous cell carcinoma (OSCC) is the most common of oral cancer and there is a need to develop alternative therapeutic strategies for OSCC because existing cancer treatment strategies such as surgery, radiation, and chemotherapy have limitations in their application due to damage to healthy tissue, dysfunction, and cosmetic problems caused by facial deformation.<sup>11,12</sup> In this study, the therapeutic effect of action of PDT using synthetic photosensitizer Pa was examined in the OSCC cell line as well as the mechanism of action. Our results showed that, in OSCC cell lines, Pa-PDT induces apoptosis via the ER stress pathway, while the ER stress affects autophagy as well.

## Materials and methods

### Preparation of synthesized pheophorbide a

Pa was synthesized according to the procedure described previously.<sup>6</sup> Briefly, the removing of a  $Mg^{2+}$  ion from chlorophyll-a and hydrolysis with 80% TFA to afford Pa as a fine powder.

### Cell culture and reagents

The human OSCC cell lines, FaDu and YD-10B cells were purchased from Korea Cell Line Bank (KCLB, Seoul, Korea). The murine OSCC cell lines, AT-84 cells were provided by Dr. E. J. Shillitoe (State University of New York, Upstate Medical University). The FaDu cell line was cultured in MEM medium (Welgene, Inc., Daegu, Korea) and the YD-10B and AT-84 cell line was cultured in RPMI 1640 medium (Welgene). The cells were maintained as monolayers at 37 °C in culture medium containing 10% heat-inactivated fetal bovine serum (FBS; Gibco, Rockville, MD, USA) and 1% penicillin / streptomycin (Gibco) in an atmosphere containing 5%  $CO_2$ /air. ER stress inhibitor PBA were purchased from sigma-aldrich (Darmstadt, Germany). The general mechanism of 4-PBA is that the hydrophobic regions of the chaperone interact with exposed hydrophobic segments of the unfolded protein.<sup>13</sup>

### Photodynamic treatment

The cells were incubated in a serum-free culture medium with Pa for 2 h. After washing, the cells were exposed with a light dose of 1.25 J/cm<sup>2</sup> performed using a light-emitting diode (LED; Philips Luxeon Lumileds, San Jose, CA, USA). This source emitted light at wavelengths 613–645 nm. A peak at 635 nm measured with a Delta Ohm DO 9721 quantum photo-radiometer and thermometer data logger (Model DO9721, Padua, Italy) was characterized as 35 mW/cm<sup>2</sup>.

### MTT assay

The cells were seeded in a 12-well plate and incubated overnight. After Pa-PDT treatment for 24 h, 0.5 ml of cell culture medium and 50  $\mu$ l of 3-(4,5-dimethylthiazol-2-yl)-3,5-diphenyltetrazolium bromide solution (MTT; AMRESCO, Fountain Pkwy, Solon, OH, USA) (0.5 mg/ml in PBS) were added to each well. After 4 h of incubation at 37 °C, the

medium was removed and formazan crystals were dissolved in 1 ml of dimethyl sulfoxide (DMSO) at room temperature for 10 min with gentle agitation. The absorbance was measured at 595 nm using Microplate Autoreader ELISA (TECAN, Männedorf, Switzerland), and all experiments were performed in triplicate.

### Western blot analysis

Western blot analysis were performed as described previously.<sup>14</sup> Antibodies were as follows: cleaved caspase-3, cleaved caspase-7, caspase-7, PARP, Beclin1, ATG5, ATG12, LC3B (Cell Signaling, Danvers, MA, USA), and Bcl-2, p-IRE1 $\alpha$ , p-PERK, ATF6, Bip, CHOP, caspase-12, and actin (Santa Cruz Biotechnology, CA, USA). Finally, the membranes were visualized with the enhanced chemiluminescence (ECL) kit (Amersham, Cardiff, UK) using the LAS-3000 Image Reader of Luminescence Image Analyzer (FUJIFILM Life Science, Tokyo, Japan). The protein levels were quantified using Multi gauge V3.0 software program (FUJIFILM Life Science) and were normalized to the expression of the actin levels.

### Reverse transcription-polymerase chain reaction (RT-PCR)

Total RNA was extracted from cells using TRIzol Reagent (Invitrogen, Carlsbad, CA, USA). 1 mg of total RNA was reverse transcribed into complementary DNA (cDNA) and 2  $\mu$ l cDNA was amplified by using the Superscript™ One-step RT-PCR with platinum® Taq kit (Invitrogen). The following primer sets were used: Human CHOP (F: 5'-AAACA-GAATCGGGTCCACTG -3', R: 5'-TGTGACCTCTGCTGGTTCTG-3'); GAPDH (F: 5'-CCAAGGTCATCCATGACAACTTTG-3', R: 5'-GTCATACCAGGAAATGAGCTTGACA-3'). The cycling conditions were as follows: The amplifications were performed at 94 °C 3 min, 35 cycles after an initial denaturation at 94 °C 30 s, annealed at 55 °C 30 s, extended at 72 °C 30 s, and extended at 72 °C 10 min in all primers. PCR products were then electrophoresed on a 1.5% agarose gel and visualized using a gel documentation system (Bio-rad, Hercules, CA, USA).

### Detection of acidic vesicular organelles (AVOs)

Acridin orange stained were performed as described previously.<sup>14</sup> Briefly, the Pa-PDT treated cells were stained with acridine orange (1  $\mu$ g/ml; Sigma–Aldrich) for 15 min. The samples were washed twice with PBS and then examined under a fluorescence microscope (Opinity, China).

### Animals and intratumoral Pa-PDT for in vivo study

AT-84 cells were used for in vivo experiments previously established by Pang et al.<sup>15</sup> Male immunocompetent C3H mice of 5 weeks of age (Samtaco, Sunghnam, South Korea) were inoculated subcutaneously on the right flank with  $1 \times 10^7$  AT-84 cells. 1 week later the tumor inoculation, Pa was administered intratumorally with 10 mg/kg body weight.

After 2 h, PDT was performed using a LED with a light dose of 100 J/cm<sup>2</sup>. The growth of the tumors was monitored daily during the following 2 weeks. Animal care and all experiments were conducted under protocols approved by the Animal Care and Use Committee at Wonkwang University, Department of Dentistry.

### Histopathology, TUNEL assay, and immunohistochemistry

The animals were euthanized on day 14 and the tumors were carefully removed and fixed in 10% formalin over 24 h. Preparation for paraffin blocks was performed as described previously.<sup>16</sup> From each block, prepared 4- $\mu$ m-thick sections were stained with hematoxylin and eosin (H&E) for histological examination. Apoptotic cells were detected the terminal deoxynucleotidyl transferase (TdT)-mediated dUTP nick end labeling (TUNEL) method using an Apoptosis Detection Kit (Millipore, Billerica, Ma, USA) according to the manufacturer's protocol. For immunohistochemistry, the sections were incubated in 3% H<sub>2</sub>O<sub>2</sub> in methanol for 10 min to remove endogenous peroxidase and blocked with 1% BSA in PBS for 1 h. The sections were then incubated with PCNA (Dako, Carpinteria, CA, USA), LC3B, Beclin1 (Cell Signaling, Danvers, MA, USA), and p62, CHOP, p-PERK, ATF6 (Santa Cruz Biotechnology, CA, USA) overnight at 4 °C. After washed three times with PBS, avidin-biotin peroxidase complex (ABC) method (Vector, Burlingame, CA, USA), and peroxidase activity was evaluated with 3,3'-diaminobenzidine (Vector, Burlingame, CA, USA). Finally, the sections were counterstained with hematoxylin.

### Statistical analysis

Data are expressed as the mean  $\pm$  SD of at least three individual experiments. Statistical comparisons between groups were performed using two-tailed Student's *t*-test (Excel, Microsoft). Statistical significance was set at \**p* < 0.05; \*\**p* < 0.01; \*\*\**p* < 0.001.

## Results

### Pa-PDT inhibited cell proliferation in human OSCC cells

The effect of Pa-PDT on cell proliferation was assessed in FaDu and YD-10B cells using MTT assay. The cells were treated Pa-PDT with various doses (0.05, 0.1, 0.2 and 0.5  $\mu$ M) for 24 h. Pa-PDT significantly inhibited the proliferation of human OSCC cells in a dose-dependent manner. In FaDu cells, Pa doses of 0.05–0.5  $\mu$ M with light resulted in cell growth inhibition rates of 36.7–86.5%, respectively (Fig. 1A). Similarly, Pa-PDT also induced significant cytotoxicity in YD-10B cells in a Pa-dose-dependent manner (Fig. 1B). The IC<sub>50</sub> value for Pa-PDT was 0.1  $\mu$ M in FaDu and YD-10B cells. There was no significant decrease in cell proliferation due to Pa or light alone in either cell line (data not shown). These results demonstrated that Pa-PDT exerts an anti-proliferative effect on human OSCC cells.

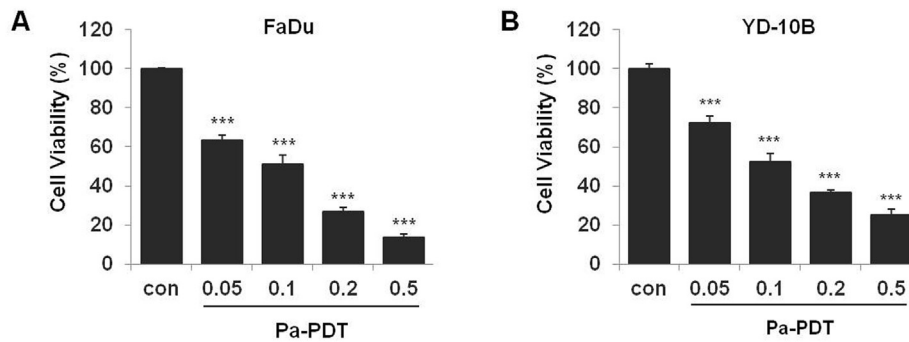


**Figure 1** The effects of Pa-PDT on proliferation in human OSCC cells. (A and B) FaDu and YD-10B cells were preincubated with various Pa concentrations (0.05–0.5  $\mu\text{M}$ ) for 2 h and then illuminated (1.25  $\text{J}/\text{cm}^2$ ). The levels of cell proliferation were measured using an MTT assay at 24h after Pa-PDT treatment. The percentage of viable cells was calculated as the ratio of treated cells to the control cells. The data are reported as the mean  $\pm$  SD of three independent experiments. \* $p < 0.05$ , \*\* $p < 0.01$ , \*\*\* $p < 0.001$  compared with the control group.

### Pa-PDT induced apoptosis and autophagy

To determine whether Pa-PDT induces apoptosis, the expression levels of apoptosis-related proteins were measured by Western blot. As shown in Fig. 2A, Pa-PDT induced the decrease of Bcl-2 and caspase-7 and the increase of cleaved caspase-3, the activated form of caspase-3. Pa-PDT also increased the level of PARP cleavage, which is known as important hallmark of apoptosis by caspases

activation in both cell lines. These results indicated that Pa-PDT induced caspase-dependent apoptosis in human OSCC cells. Induction of autophagy by Pa-PDT was next determined by assessing the levels of Beclin1, ATG5, ATG12 and LC3B-I/II, which play a crucial role in autophagy, in human OSCC cells using Western blot. Pa-PDT dose-dependently increased the levels of Beclin1, ATG5 and LC3-II, whereas the expression of ATG12 was not significant expression in human OSCC cells (Fig. 2B). This finding

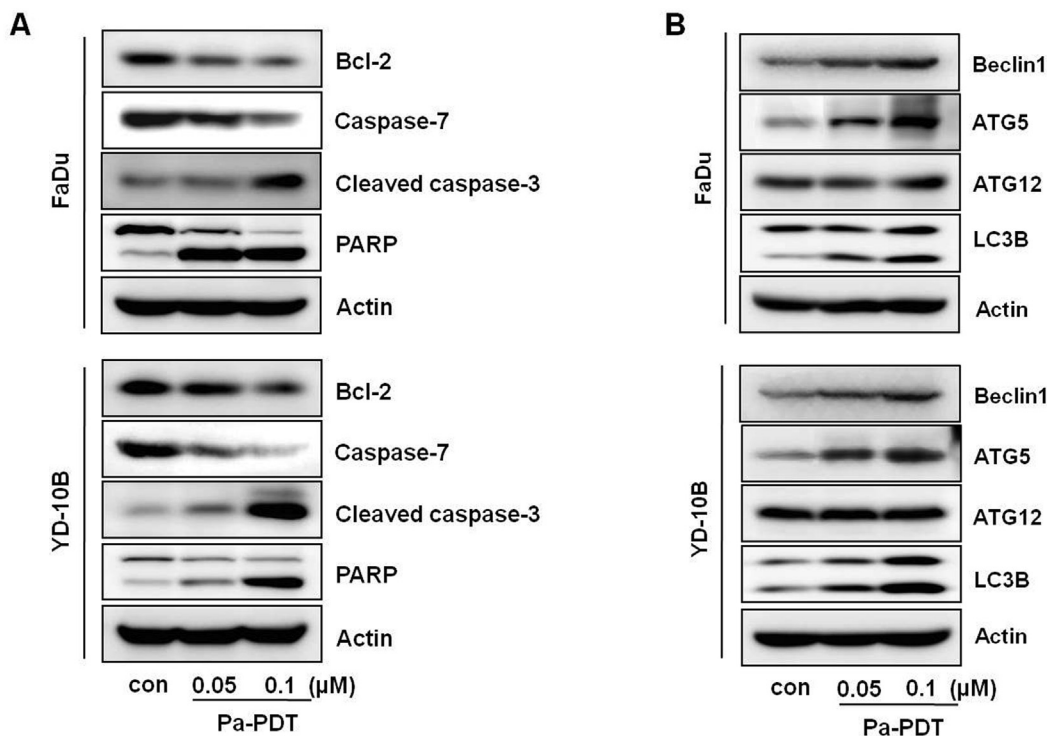


**Figure 2** Apoptosis and autophagy analysis of Pa-PDT treated human OSCC cells. (A) Expression of apoptosis-related proteins in Pa-PDT treated cells. (B) Expression of autophagy-related proteins in Pa-PDT treated cells. FaDu and YD-10B cells were treated with Pa-PDT for 24 h at indicated concentration. The total cell lysates were prepared and the protein was subjected to SDS-PAGE followed by Western blot analysis and chemiluminescent detection. Western blot analysis was performed using a series of antibodies; Bcl-2, caspase-7, cleaved caspase-3, PARP, Beclin1, ATG5, ATG12 and LC3B. The protein levels were normalized by a comparison to the actin levels.

indicated that Pa-PDT induced not only apoptosis, but also autophagy in human OSCC cells.

### Pa-PDT induced ER stress in human OSCC cells

This study next assessed whether Pa-PDT induces ER stress in human OSCC cells. The ER stress response to Pa-PDT was examined using RT-PCR, and marked induction of CHOP expression was observed in Pa-PDT treatment (Fig. 3A). Western blot was next performed to confirm the expression levels of ER stress-related proteins. As shown in Fig. 3B, the protein expression levels of CHOP and caspase-12 also increased in Pa-PDT treatment. Pa-PDT increased protein expression levels of p-IRE1 $\alpha$ , p-PERK, ATF6, and Bip compared with the control group (Fig. 3C). These results showed that Pa-PDT induced ER stress in human OSCC cells.

### Inhibition of ER stress by PBA in Pa-PDT treated cells

We determined whether ER stress inhibitor PBA could inhibit Pa-PDT-induced ER-stress in human OSCC cells. The levels of ER stress-related expression were examined using RT-PCR and Western blot. As shown in Fig. 4A, PBA effectively inhibited Pa-PDT-induced CHOP expression in human OSCC cells. The protein levels of CHOP and caspase-12 expression were also inhibited by PBA in Pa-PDT treated FaDu and YD-10B cells (Fig. 4B). Cell viability was next examined using MTT assays in Pa-PDT treatment with and without PBA. Pa-PDT with PBA treatment significantly recovering cell viability when compared with Pa-PDT without PBA in both FaDu and YD-10B cells (Fig. 4C). These results showed that ER stress induced by Pa-PDT was related with human OSCC cells death.

### Involvement of ER stress in Pa-PDT induced apoptosis and autophagy

To investigate potential cross-talk between ER stress and the induction of apoptosis and autophagy in response to Pa-PDT, we next examined whether ER stress inhibitor PBA could regulate Pa-PDT-induced apoptosis or autophagy in human OSCC cells. The levels of apoptosis-related proteins expression were examined using Western blot in Pa-PDT treatment with PBA. As shown in Fig. 5A, Pa-PDT-induced cleaved caspase-7 and PARP cleavage were inhibited by PBA in FaDu and YD-10B cells. The result showed that the inhibition of ER stress plays a vital role in Pa-PDT induced apoptosis. We next examined the expression levels of a key autophagy protein, LC3B, during treatment with the ER stress inhibitor PBA using Western blot. Pretreatment of cells with the ER stress inhibitor PBA significantly increased Pa-PDT-induced expression of LC3B proteins in FaDu and YD-10B cells (Fig. 5B). The autophagy response to PBA in Pa-PDT-treated cells was next confirmed using acridine orange staining. Within acidic vesicles by autophagy, acridine orange becomes protonated and trapped within the organelle and forms aggregates that emit bright red fluorescence.<sup>17</sup> As shown in Fig. 5C, Pa-PDT increased the intensity of red fluorescence in both cells. Additionally, pretreatment of 1 mM PBA strongly increased the formation of Pa-PDT-induced AVO. These results indicated that ER stress is involved in Pa-PDT-induced autophagy in human OSCC cells.

### In vivo study on IT Pa-PDT on AT-84 cells bearing CH3 mice

Effect of IT Pa-PDT on tumor growth in vivo was examined using mice inoculated with AT-84 cells. IT Pa-PDT

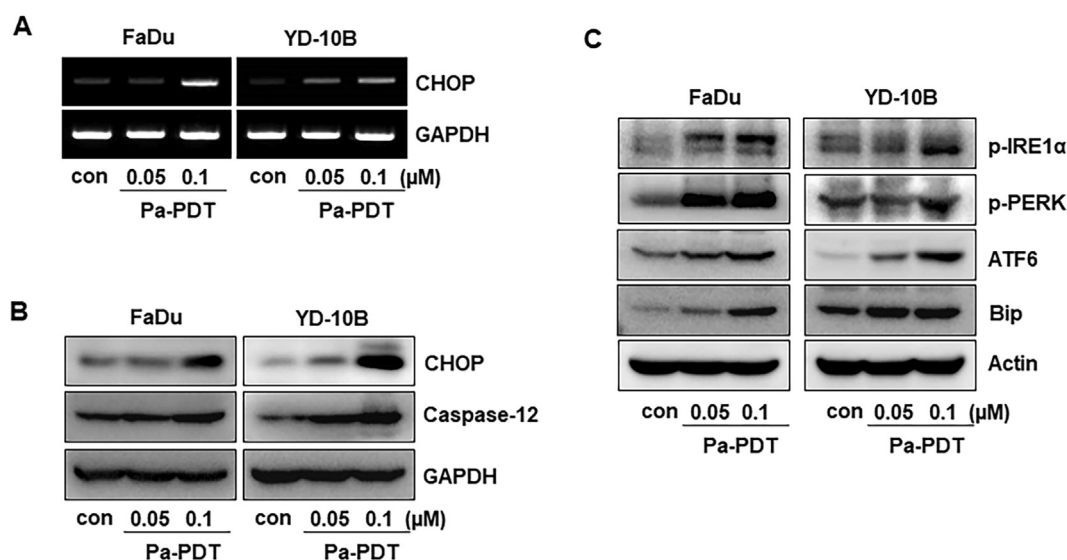


**Figure 3** Induction of ER stress in Pa-PDT-treated human OSCC cells. (A) The mRNA expression levels of CHOP in Pa-PDT treated cells. mRNA was isolated and RT-PCR was performed. The PCR products were separated on 1.5% agarose gels and values were normalized by comparing to the GAPDH. (B) Expression of ER stress-related proteins in Pa-PDT treated cells. (C) Expression of ER stress-induced cell death-related proteins in Pa-PDT treated cells. FaDu and YD-10B cells were treated with Pa-PDT for 24 h at indicated concentration. Cell lysates were subjected to Western blot analysis using antibodies; CHOP, caspase-12, p-IRE1 $\alpha$ , p-PERK, ATF6 and Bip. The protein levels were normalized by comparing to the actin levels.

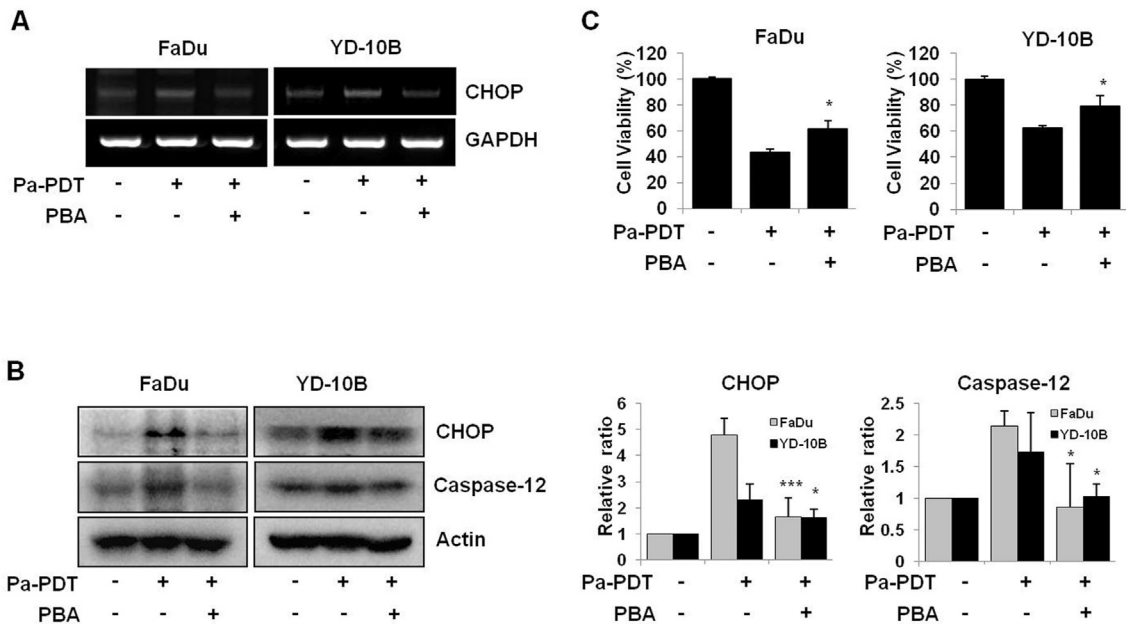


**Figure 4** Inhibition of ER stress by 4-phenylbutyrate (PBA) in Pa-PDT-treated human OSCC cells. The cells were treated with Pa-PDT for 24 h in the presence or absence of PBA (1 mM). (A) The mRNA expression levels of CHOP in Pa-PDT and PBA co-treated cells. mRNA was isolated and RT-PCR was performed. The PCR products were separated on 1.5% agarose gels and values were normalized by comparing to the GAPDH. (B) Western blot analysis was performed using ER stress-related proteins antibodies (CHOP, caspase-12) in cells co-treated with Pa-PDT with PBA. The protein levels were normalized by a comparison with the actin levels. The relative ratio in expressed protein was assessed by scanning densitometry. The data are reported as the mean  $\pm$  SD of three independent experiments. \* $p < 0.05$ , \*\* $p < 0.01$ , \*\*\* $p < 0.001$  compared with the Pa-PDT treated group. (C) Cell viability was determined by MTT assay after co-treated with Pa-PDT and PBA. The percentage of viable cells was calculated as the ratio of treated cells to the control cells. The data are reported as the mean  $\pm$  SD of three independent experiments. \* $p < 0.05$ , \*\* $p < 0.01$ , \*\*\* $p < 0.001$  compared with the Pa-PDT treated group.

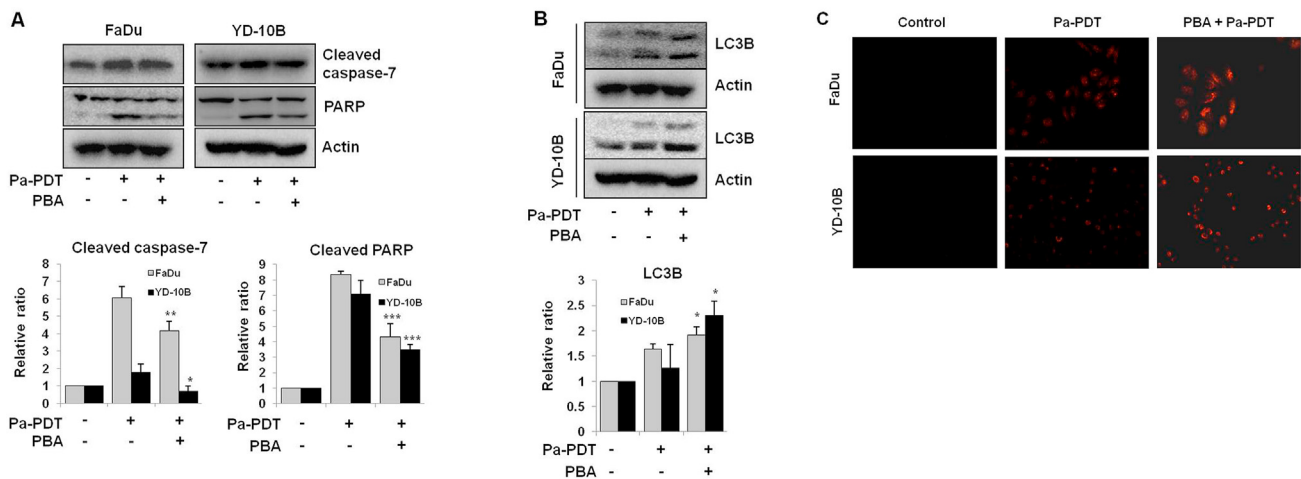


**Figure 5** Regulation of apoptosis and autophagy by the inhibition of ER stress in Pa-PDT-treated human OSCC cells. The cells were treated with Pa-PDT for 24 h in the presence or absence of PBA (1 mM). (A) Expression of apoptosis-related proteins in cells co-treated with Pa-PDT with PBA. (B) Conversion of LC3B, the autophagy marker protein after co-treated with Pa-PDT and PBA. Cell lysates were subjected to Western blot analysis using antibodies; cleaved caspase-7, PARP and LC3B. The protein levels were normalized by a comparison with the actin levels. The relative ratio in expressed protein was assessed by scanning densitometry. The data are reported as the mean  $\pm$  SD of three independent experiments. \* $p < 0.05$ , \*\* $p < 0.01$ , \*\*\* $p < 0.001$  compared with the Pa-PDT treated group. (C) The effect of PBA on Pa-PDT-induced acidic vesicular organelle (AVO) formation. After Pa-PDT treatment with PBA, acridine orange (1  $\mu$ g/ml) was added to the living cells for 30 min and the cells were visualized under a fluorescence microscope (200  $\times$  magnification).

significantly decreased tumor volume compared to the control group (Fig. 6A). Solid SCC tumor growth was observed in control group, whereas cell death with nuclear pyknosis and various small nuclear fragments was observed in IT Pa-PDT treated group (Fig. 6B). The positively stained cells for PCNA (cell proliferation marker) were strong staining detected in control group, whereas markedly decreased in IT Pa-PDT treated group. The number of apoptotic TUNEL-positive cells were increased in IT Pa-PDT treatment, compared to those in the control group (Fig. 6B). We next examined the expression of autophagy and ER stress-related protein in tumor sections using immunohistochemistry. LC3B and Beclin1 were detected in the cytoplasm of tumor after IT Pa-PDT, whereas the p62 was strongly induced in the control and its expression was inhibited by IT Pa-PDT treatment (Fig. 6C). The expression of CHOP, p-PERK and ATF6 were strongly detected in IT Pa-PDT treated group compared to control group (Fig. 6D). These results showed that IT Pa-PDT also induced apoptosis, autophagy and ER stress in vivo tumor model, consistent with the results of in vitro experiments.

## Discussion

PDT was reported to inhibit cancers through different cell death pathways, and its effectiveness is dependent on the

types of cancer cell lines and photosensitizers.<sup>18–20</sup> The action mechanism of PDT on photosensitizers might depend on the subcellular localization and molecular targets and the tumor cell type. The present study was designed to investigate the underlying mechanisms of newly synthesized Pa-PDT induced ER stress and cell death on OSCC cells.

Pa-PDT significantly inhibited cell proliferation of OSCC cells in a dose-dependent manner. We next evaluated the mode of cell death by Pa-PDT. PDT can lead to cell death via the apoptosis pathway. The decrease in Bcl-2 proteins led to the activation of caspase-3/-7 and PARP cleavage in Pa-PDT-treated cells. It suggests induced apoptotic cell death through mitochondria-dependent intrinsic pathway.

Autophagy is a homeostatic cellular recycling mechanism, but recently attracted the interest in the field of cancer research because it is designated as programmed cell death type II.<sup>21,22</sup> It is suggesting that autophagy features both the promotion and antagonization of apoptosis.<sup>23</sup> The two major proteins associated with autophagy are LC3 and Beclin1.<sup>23</sup> Among these, Beclin1 plays a tumor suppressor and is an essential mediator of autophagy, while LC3-II interacts with adaptor proteins for degradation of cellular components in the autophagolysosome.<sup>23,24</sup> In the course of autophagy, LC3-II is yielded by the combination of phosphatidylethanolamine in the presence of ATG5/ATG7/ATG12.<sup>25</sup> We next examined whether Pa-PDT induces

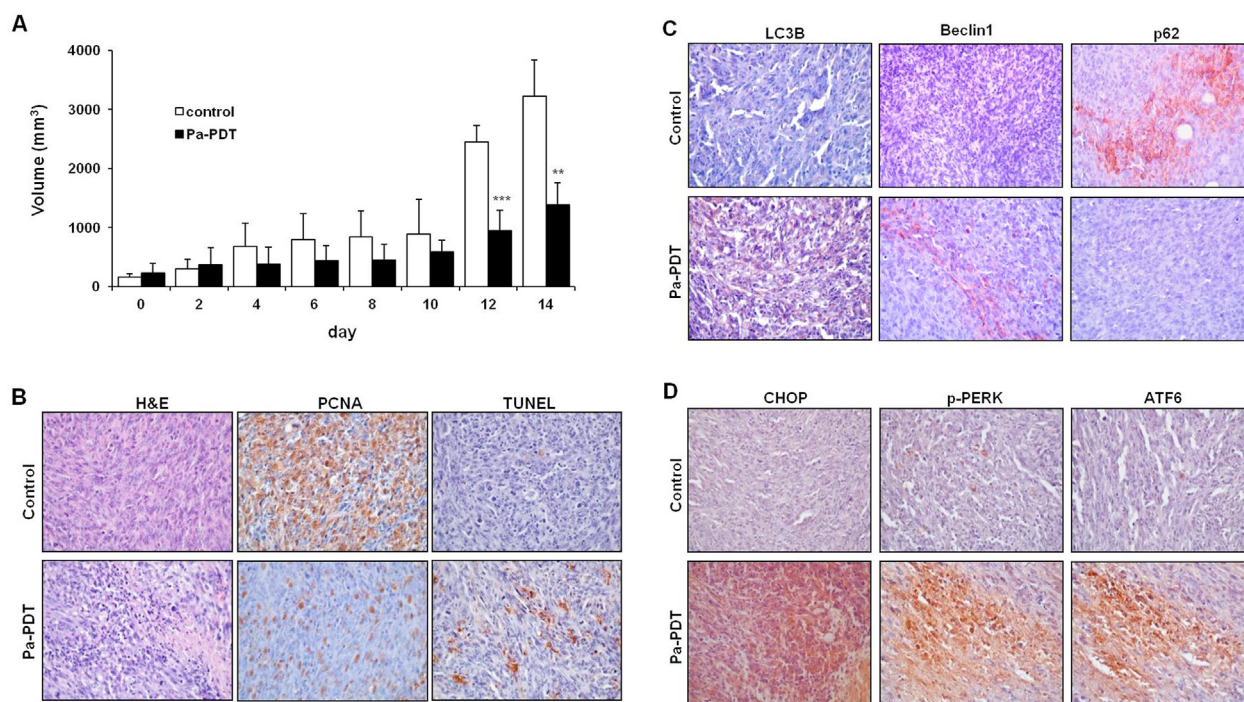


**Figure 6** Effect of IT Pa-PDT on tumor growth, apoptosis, autophagy and ER stress in vivo model. C3H mice bearing AT-84 murine oral cancer cells were treated with IT Pa-PDT. (A) Relative tumor volumes of the mice treated with IT Pa-PDT and the vehicle-treated controls. Tumor volume was measured every 2 days and calculated by the formula:  $V = (ab^2)/2$ , in which  $a$  is the longest diameter, and  $b$  is the shortest diameter of the tumor. The data are reported as the mean  $\pm$  SD of five animals. \* $p < 0.05$ , \*\* $p < 0.01$ , \*\*\* $p < 0.001$  compared with the control group. (B) H&E staining, immunohistochemistry for PCNA, TUNEL assay were performed on paraffin sections from the tumor. Immunohistochemical study for autophagy (C) and ER stress (D) were performed on paraffin sections from the tumor using antibodies; LC3B, Beclin1, p62, CHOP, p-PERK, ATF6. Photographs were taken under a magnification of  $400\times$ .

autophagy in OSCC cells. The results showed that Pa-PDT dramatically increased the levels of autophagy-related protein (Beclin1, ATG5, LC3B). Previous study identified that autophagy contributes to Pa-PDT-induced cell growth inhibition in human oral cancer cell line YD-10B cells.<sup>14</sup>

ER stress has been reported as another factor inducing apoptosis in addition to the extrinsic death receptor-induced pathway and the intrinsic/mitochondrial-mediated pathway.<sup>26</sup> The UPR is triggered in response to the accumulation of misfolded proteins in the ER. Our data showed that Pa-PDT activated the UPR through increases the expression levels of Bip, p-IRE1 $\alpha$ , p-PERK, ATF6, demonstrating ER stress induction. If the ER stress is prolonged, or ER function is perturbed, damage may be caused in cells and lead to apoptosis.<sup>27</sup> In this study, Pa-PDT treatment induced upregulated CHOP and caspase-12 expression in FaDu and YD-10B cells and strongly induced the expression levels of CHOP, p-PERK and ATF6 in AT-84-inoculated tumor tissue in vivo. Therefore, these results indicate the involvement of UPR signaling in Pa-PDT induced apoptosis.

In this work, ER stress in both autophagic and apoptotic processes were studied with regards to possible upstream pathways. In some previous studies, the involvement of the ER stress pathway in the regulation of autophagy and apoptosis has been reported.<sup>28,29</sup> We investigated whether Pa-PDT-induced ER stress leads to the activation of the apoptotic pathway. FaDu and YD-10B cells were treated with Pa-PDT in the presence or absence of PBA, specific inhibitors of the ER stress process. Pa-PDT with PBA treatment has significantly induced cell viability compared to Pa-PDT-alone treatment. This demonstrates that Pa-PDT leads to apoptosis mediated by ER stress, thus inhibiting OSCC cell growth. Moreover, autophagy of OSCC cells induced by Pa-PDT was promoted by ER stress inhibition. Autophagy is known to play a key role in ER stress relief and homeostasis recovery.<sup>30</sup> In this study, autophagy maintains cellular homeostasis by alleviating Pa-PDT-induced ER stress, it is thought that elevated levels of stress induce cell damage by apoptotic mechanisms. Interactions between ER stress and autophagy and apoptosis-related proteins have been found, but the regulatory mechanisms require further study.

In conclusion, we demonstrated that synthesized Pa-PDT induces ER stress in OSCC cells. This study also confirmed the involvement of ER stress in Pa-PDT induced apoptosis and autophagy. Therefore, Pa-PDT is a potential therapy for human oral cancer, and co-treatment with targeting ER stress may represent a novel treatment strategy against OSCC.

### Declaration of competing interest

The authors have no conflicts of interest relevant to this article.

### Acknowledgements

This study was supported by Basic Science Research Program through the National Research Foundation of Korea (NRF) funded by the Ministry of Education, Science and

Technology, South Korea (No. NRF-2018R1A6A3A11050958, No. NRF-2016R1D1A1B01006388, No. NRF-2014R1 A1A200 9007).

### References

- Karakullukcu B, Nyst HJ, van Veen RL, et al. mTHPC mediated interstitial photodynamic therapy of recurrent nonmetastatic base of tongue cancers: development of a new method. *Head Neck* 2012;34:1597–606.
- D’Cruz AK, Robinson MH, Biel MA. mTHPC-mediated photodynamic therapy in patients with advanced, incurable head and neck cancer: a multicenter study of 128 patients. *Head Neck* 2004;26:232–40.
- Hopper C, Kübler A, Lewis H, Tan IB, Putnam G. mTHPC mediated photodynamic therapy for early oral squamous cell carcinoma. *Int J Cancer* 2004;111:138–46.
- Leung WN, Sun X, Mak NK, Yow CM. Photodynamic effects of mTHPC on human colon adenocarcinoma cells: photocytotoxicity, subcellular localization and apoptosis. *Photochem Photobiol* 2002;75:406–11.
- Paszko E, Ehrhardt C, Senge MO, Kelleher DP, Reynolds JV. Nanodrug applications in photodynamic therapy. *Photo-diagnosis Photodyn Ther* 2011;8:14–29.
- You H, Yoon HE, Yoon JH, Ko H, Kim YC. Synthesis of pheophorbide-a conjugates with anticancer drugs as potential cancer diagnostic and therapeutic agents. *Bioorg Med Chem* 2011;19:5383–91.
- Kroeger H, Chiang WC, Felden J, Nguyen A, Lin JH. ER stress and unfolded protein response in ocular health and disease. *FEBS J* 2019;286:399–412.
- Simmen T, Herrera-Cruz MS. Plastic mitochondria-endoplasmic reticulum (ER) contacts use chaperones and tethers to mould their structure and signaling. *Curr Opin Cell Biol* 2018;53:61–9.
- Yoo YS, Han HG, Jeon YJ. Unfolded protein response of the endoplasmic reticulum in tumor progression and immunogenicity. *Oxid Med Cell Longev* 2017;2017:2969271.
- Shaheen A. Effect of the unfolded protein response on ER protein export: a potential new mechanism to relieve ER stress. *Cell Stress Chaperones* 2018;23:797–806.
- Cho K, Wang X, Nie S, Chen Z, Shin DM. Therapeutic nanoparticles for drug delivery in cancer. *Clin Cancer Res* 2008;14:1310–6.
- Wong HL, Bendaya R, Rauth AM, Li Y, Wu XY. Chemotherapy with anticancer drugs encapsulated in solid lipid nanoparticles. *Adv Drug Deliv Rev* 2007;59:491–504.
- Pao HP, Liao WI, Wu SY, Huang KL, Chu SJ. Suppression of endoplasmic reticulum stress by 4-PBA protects against hyperoxia-induced acute lung injury via up-regulating claudin-4 expression. *Front Immunol* 2021;12:674316.
- Ahn MY, Yoon HE, Kwon SM, et al. Synthesized pheophorbide a-mediated photodynamic therapy induced apoptosis and autophagy in human oral squamous carcinoma cells. *J Oral Pathol Med* 2013;42:17–25.
- Pang S, Kang MK, Kung S, et al. Anticancer effect of a lentiviral vector capable of expressing HIV-1 Vpr. *Clin Cancer Res* 2001;7:3567–73.
- Ahn MY, Yoon HE, Moon SY, Kim YC, Yoon JH. Intratumoral photodynamic therapy with newly synthesized pheophorbide a in murine oral cancer. *Oncology Research* 2017;25:295–304.
- Sengottuvelan M, Ravi KA. Methods for studying autophagy within the tumor microenvironment. *Adv Exp Med Biol* 2016;899:145–66.
- Dolmans DE, Fukumura D, Jain R. Photodynamic therapy for cancer. *Nat Rev Cancer* 2003;3:380–7.
- Baldea I, Filip AG. Photodynamic therapy in melanoma- an update. *J Physiol Pharmacol* 2012;63:109–18.

20. Buytaert E, Dewaele M, Agostinis P. Molecular effectors of multiple cell death pathways initiated by photodynamic therapy. *Biochim Biophys Acta* 2007;1776:86–107.
21. Janku F, McConkey DJ, Hong DS, Kurzrock R. Autophagy as a target for anticancer therapy. *Nat Rev Clin Oncol* 2011;8: 528–39.
22. Bursch W, Ellinger A, Gerner C, Frohwein U, Schulte-Hermann R. Programmed cell death (PCD). Apoptosis, autophagic PCD, or others? *Ann N Y Acad Sci* 2000;926:1–12.
23. Yu L, Chen Y, Tooze SA. Autophagy pathway: cellular and molecular mechanisms. *Autophagy* 2018;14:207–15.
24. Schille S, Crauwels P, Bohn R, et al. LC3-associated phagocytosis in microbial pathogenesis. *Int J Med Microbiol* 2017;4221: 30283–7.
25. Ahn MY, Ahn SG, Yoon JH. Apicidin, a histone deacetylase inhibitor, induces both apoptosis and autophagy in human oral squamous carcinoma cells. *Oral Oncol* 2011;47:1032–8.
26. Cao Y, Long J, Liu L, et al. A review of endoplasmic reticulum (ER) stress and nanoparticle (NP) exposure. *Life Sci* 2017;186:33–42.
27. Li X, Meng L, Wang F, Hu X, Yu Y. Sodium fluoride induces apoptosis and autophagy via the endoplasmic reticulum stress pathway in MC3T3-E1 osteoblastic cells. *Mol Cell Biochem* 2018;454:77–85.
28. Demirtas L, Guclu A, Erdur FM, et al. Apoptosis, autophagy & endoplasmic reticulum stress in diabetes mellitus. *Indian J Med Res* 2016;144:515–24.
29. Chiang CK, Wang CC, Lu TF, et al. Involvement of endoplasmic reticulum stress, autophagy, and apoptosis in advanced glycation end products-induced glomerular mesangial cell injury. *Sci Rep* 2016;6:34167.
30. Hooper KM, Barlow PG, Henderson P, Stevens C. Interactions between autophagy and the unfolded protein response: implications for inflammatory bowel disease. *Inflamm Bowel Dis* 2019;25:661–71.